ELSEVIER

Journal of Power Sources 83 (1999) 156–161

JOURNAL OF POWER SOURCES

www.elsevier.com/locate/jpowsour

Spinel $Li[Li_{1/3}Ti_{5/3}]O_4$ as an anode material for lithium ion batteries

G.X. Wang *, D.H. Bradhurst, S.X. Dou, H.K. Liu

Energy Storage Materials Program, Institute for Superconducting and Electronic Materials, University of Wollongong, Wollongong, NSW 2522, Australia

Received 2 December 1998; received in revised form 8 April 1999; accepted 27 April 1999

Abstract

The spinel $Li[Li_{1/3}Ti_{5/3}]O_4$ compound was synthesised via a solid-state method and its electrochemical performance in lithium ion cells was examined. Lithium ions intercalate into and deintercalate from $Li[Li_{1/3}Ti_{5/3}]O_4$ with high reversibility. The spinel $Li[Li_{1/3}Ti_{5/3}]O_4$ demonstrated a very stable structural characteristic for lithium ion insertion and extraction without passivation on its surface. The spinel $Li[Li_{1/3}Ti_{5/3}]O_4$ as an anode material was coupled with $LiCoO_2$ and $LiMn_2O_4$ as cathodes to construct lithium ion cells. These cells provide 2.4–2.5 V operating voltage and without the safety concerns associated with using lithium metal or carbon anodes.

Keywords: Spinel $Li[Li_{1/3}Ti_{5/3}]O_4$; Lithium ion battery; Chemical insertion; AC impedance spectroscopy

1. Introduction

Intercalation electrode materials for lithium ion batteries have been extensively investigated worldwide in the past 20 years [1,2]. TiS_2, MoS_2 and MnO_2 were initially chosen as cathode materials and coupled with lithium metal as anode [3–5]. Such rechargeable systems failed to be commercialised due to safety concerns because of the internal short circuits caused by lithium dendrites and the reaction of high surface area lithium powders formed by cycling. Recently, ''rocking-chair'' or ''lithium ion batteries'' have been developed using layered $LiCoO_2$, $LiNiO_2$ and spinel $LiMn_2O_4$ as cathode and carbonaceous materials as anode [6–9]. Lithium ions shuttle between the cathode and anode hosts. However, the main drawback for carbonaceous materials is the passivation film formed during the first charging, which consumes lithium from the cathode [10–12]. This passivation layer could decompose at higher temperature, inducing failure of the cell and even ignition of the battery. The safety concern still exists.

Spinel materials of the type $Li[M_2]O_4$ have a cubic symmetry $Fd\bar{3}m$ which provides a three dimensional tunnel for lithium diffusion. The strong M–O bond maintains the $[M_2]O_4$ framework during lithium insertion and extraction [13]. The defect spinels $Li[Li_{1/3}M_{5/3}]O_4$ (M=Mn, Ti) are extremely tolerant to cycling because the volume of the cubic unit cell changes less than 1% [14]. $Li[Li_{1/3}Ti_{5/3}]O_4$ has been identified by Ohzuku et al. as a zero-strain insertion material with excellent cyclability [15]. However, there is no detailed report on the investigation of the kinetic process of the $Li[Li_{1/3}Ti_{5/3}]O_4$ electrode.

An investigation of the synthesis and electrochemical characteristics of the spinel $Li[Li_{1/3}Ti_{5/3}]O_4$ are described in this paper. Firstly, $Li[Li_{1/3}Ti_{5/3}]O_4$ was used as cathode in a $Li/Li[Li_{1/3}Ti_{5/3}]O_4$ cell. In this system, AC impedance was employed to characterise the $Li[Li_{1/3}Ti_{5/3}]O_4$ electrode. Secondly, $Li[Li_{1/3}Ti_{5/3}]O_4$ was used as anode coupled with high voltage insertion materials such as $LiCoO_2$ and $LiMn_2O_4$ to construct lithium ion cells.

2. Experimental

The spinel $Li[Li_{1/3}Ti_{5/3}]O_4$ was synthesised by two methods. The first required heating stoichiometric TiO_2 (99.99%, Aldrich) and LiOH. H_2O (99%, Aldrich) at 850°C for 20 h under an oxygen stream. The second involved heating precursors

* Corresponding author. Tel.: +61-2-42-215765; fax: +61-2-42-215731; E-mail: guoxiu@uow.edu.au

0378-7753/99/$ - see front matter
PII: S0378-7753(99)00290-6

at 1000°C for 20 h in air, providing 8 mol% excess Li to compensate for the loss of Li_2O at high temperature. X-ray diffraction (XRD) was performed on the synthesised spinel powders using a Phillips PW1010 diffractometer with Cu–Kα radiation. The lattice constants were refined against an internal silicon standard.

CR2032 coin cells were constructed to determine the electrochemical characteristics of the spinel. The cells were assembled in an argon filled glove-box (Unilab, MBRAUN, USA), in which the moisture and oxygen was strictly controlled to less than 1 ppm. For the $Li/Li[Li_{1/3}Ti_{5/3}]O_4$ cell, lithium foil (0.38 mm thick) was used as anode and the spinel $Li[Li_{1/3}Ti_{5/3}]O_4$ was used as cathode. The cathode was a mixture of 85 wt.% active materials, 10 wt.% carbon black and 5 wt.% Polyvinylidene fluoride (PVdF) binder dispersed into dimethyl phthalate (DMP) to obtain a slurry. The slurry was spread on to an aluminium foil discs ($\phi = 18$ mm) and then dried at 200°C for 48 h. The thickness of the active materials was about 100 μm. The electrolyte was 1 M $LiPF_6$ dissolved in the mixture of EC (ethylene carbonate) and DMC (dimethyl carbonate) (1:1 by volume). The spinel $Li[Li_{1/3}Ti_{5/3}]O_4$ was also used as anode coupled with $LiCoO_2$ and $LiMn_2O_4$ to fabricate lithium ion cells. The $LiCoO_2$ was obtained from Union Minere (Belgium). $LiMn_2O_4$ spinel was prepared by reacting the stoichiometric Li_2CO_3 and Mn_2O_3 at high temperature. The details of the preparation were as described previously [16]. The cells were cycled at a constant current density of 0.15 mA/cm^2. AC impedance was employed to characterise the $Li[Li_{1/3}Ti_{5/3}]O_4$ electrode using an EG&G Princeton Applied Research Electrochemical Impedance Analyser (Model 6310). The a.c. amplitude was 5 mV, and frequency range was 100 kHz–0.01 Hz.

3. Results and discussion

3.1. Structural characterisation of $Li_4Ti_5O_{12}$

Fig. 1 shows the X-ray patterns of $Li[Li_{1/3}Ti_{5/3}]O_4$ synthesised by two different methods. The $Li[Li_{1/3}Ti_{5/3}]O_4$ synthesised at 1000°C with 8 mol% excess Li contained an impurity phase which was identified to be Li_2TiO_3. The single phase $Li[Li_{1/3}Ti_{5/3}]O_4$ compound was obtained by heating stoichiometric precursor materials at 850°C under an oxygen stream. This sample was chosen to fabricate electrodes for lithium test cells. All diffraction peaks were indexed assuming a face-centered cubic system ($Fd\bar{3}m$ space group). Lithium ions are at 8a tetrahedral sites. Lithium ions and titanium ions are located at octahedral 16d sites with ratio Li:Ti = 1:5, and oxygen ions are at 32e sites. Thus, $Li[Li_{1/3}Ti_{5/3}]O_4$ could be expressed as $[Li]_{8a}[Li_{1/3}Ti_{5/3}]_{16d}[O_4]_{32e}$ in space notation. The lattice constant was calculated to be $a = 8.364$ Å, which is

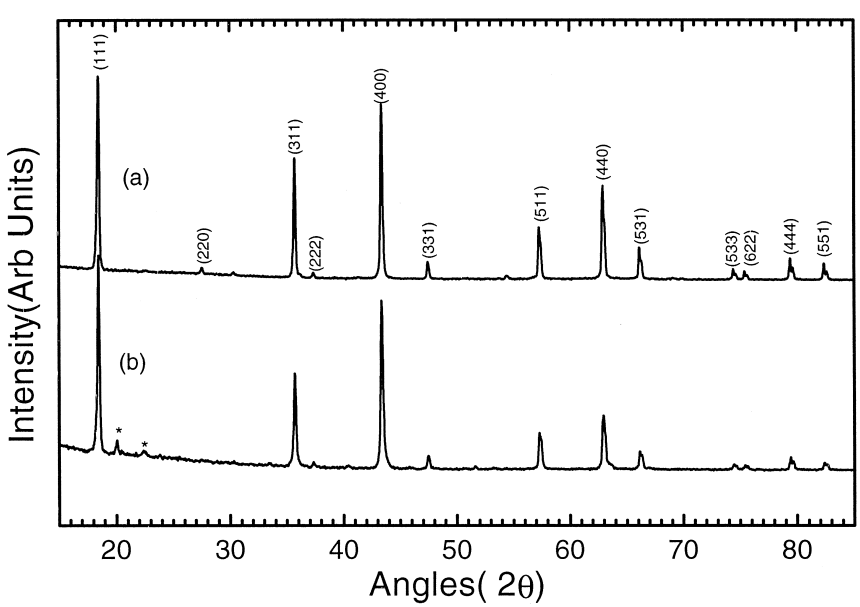

Fig. 1. X-ray diffraction patterns of $Li[Li_{1/3}Ti_{5/3}]O_4$: (a) synthesised at 850°C under oxygen stream; (b) synthesised at 1000° in air with 8 mol% Li in the precursors. * Impurity phase Li_2TiO_3.

in agreement with previous work by Murphy et al. [17]. Each formula $Li[Li_{1/3}Ti_{5/3}]O_4$ can accommodate one lithium ion. Ohzuku et al. [15] described the process of the insertion of Li ions into $Li[Li_{1/3}Ti_{5/3}]O_4$ spinel structure as follows:

$$[Li]_{8a}[Li_{1/3}Ti_{5/3}]_{16d}[O4]_{32e} + e^- + xLi^+ \quad \rightleftarrows [Li_{1+x}]_{8a/16c}[Li_{1/3}Ti_{5/3}]_{16d}[O_4]_{32e} \rightleftarrows [Li_2]_{16c}[Li_{1/3}Ti_{5/3}]_{16d}[O_4]_{32e} \quad (1)$$

During the intercalation of Li ions into the $Li[Li_{1/3}Ti_{5/3}]O_4$ structure, Li ions begin to occupy 16c sites. Then Li ions in the tetrahedral 8a sites also migrate to 16c sites. Eventually, all 16c sites are occupied by Li ions. The insertion product $Li_2[Li_{1/3}Ti_{5/3}]O_4$ is still cubic spinel phase. In order to confirm this mechanism, chemical lithium intercalation into $Li[Li_{1/3}Ti_{5/3}]O_4$ was carried out by reacting $Li[Li_{1/3}Ti_{5/3}]O_4$ powders with 2.5 M *n*-butyllithium in a hexane solution in a glove-box filled with argon. The samples were immersed in butyllithium-hexane solution for different times, then filtered and washed with hexane. The XRD was performed on these chemical insertion products which were sealed in two pieces of glass with wax in the glove-box. The content of lithium ions inserted into the sample was determined by atomic absorption spectrophotometry. As shown in Fig. 2, the insertion products $Li_{1+x}[Li_{1/3}Ti_{5/3}]O_4$ retain the cubic phase. The impurity phase marked in Fig. 2 could be unfiltered butyllithium or other ternary Li–Ti–O phases, but they are difficult to identify by XRD. After long term chemical insertion, the maximum amount of Li ions which can be inserted into the structure of the $Li[Li_{1/3}Ti_{5/3}]O_4$ is limited to about one Li ion per formula $Li[Li_{1/3}Ti_{5/3}]O_4$. This is because there are no vacant octahedral sites available to further accommodate Li ions [15]. According to the reaction (1), the $Li[Li_{1/3}Ti_{5/3}]O_4$ compound has a theoretical capacity of 175 mAh/g.

3.2. Electrochemical test of the $Li[Li_{1/3}Ti_{5/3}]O_4$ electrode

$Li/Li[Li_{1/3}Ti_{5/3}]O_4$ coin cells were constructed to examine the electrochemical performance of the $Li[Li_{1/3}Ti_{5/3}]O_4$ electrode in lithium cells. Fig. 3 shows the charge/discharge profiles of one of these cells. The cells were cycled between 1.2 V and 3.2 V. The average discharge voltage is around 1.5 V, while the charge plateau is around 1.54 V. There is about 40 mV hysteresis between the charge and discharge plateaus, which is different from the observation of Ohzuku et al. [15]. It is probably caused by the different synthesis processes. A rechargeable capacity of approximately 150 mAh/g was obtained, corresponding to 0.86 Li, which can be reversibly intercalated and de-intercalated in per formula $Li[Li_{1/3}Ti_{5/3}]O_4$. In the first hundred cycles, the capacity of $Li[Li_{1/3}Ti_{5/3}]O_4$ electrode was almost constant, indicating that $Li[Li_{1/3}Ti_{5/3}]O_4$ structure is very stable for Li ion insertion and extraction. Fig. 4 shows the differential chronopotentiometric curves of dQ/dV vs. E for the first cycle and the hundredth cycle. The oxidation peak and reduction peak are at 1.55 V and 1.50 V, respectively, which is in agreement with the data from the charge and discharge plateaus.

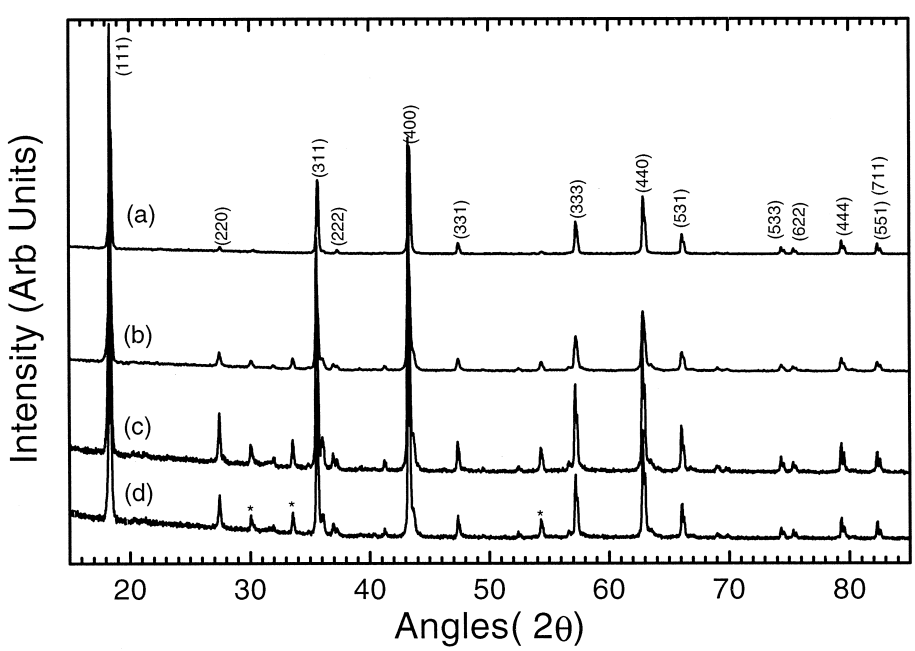

Fig. 2. XRD patterns of the chemical insertion products $Li_{1+x}[Li_{1/3}Ti_{5/3}]O_4$: (a) $x = 0$, (b) $x = 0.44$, (c) $x = 0.71$, (d) $x = 1.02$. * Impurity phases.

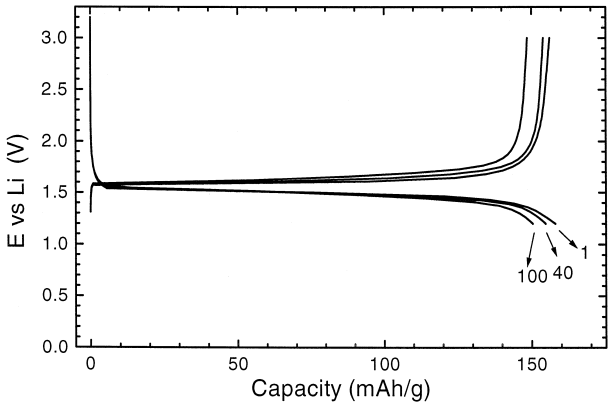

Fig. 3. The selected cycling profiles of Li/Li[$Li_{1/3}Ti_{5/3}$]O_4 cell. The cell was cycled between 1.2 V and 3.2 V at a constant current density of 0.15 mA/cm^2 which is equal to a rate of C/8.

Li[$Li_{1/3}Ti_{5/3}$]O_4 demonstrated a stable discharge plateau at 1.5 V. It can be used, therefore, as an anode material and coupled with a high voltage cathode material such as $LiCoO_2$ and spinel $LiMn_2O_4$ to construct a lithium ion cell with a voltage range of 2.4–2.5 V. The Li[$Li_{1/3}Ti_{5/3}$]O_4/$LiCoO_2$ and Li[$Li_{1/3}Ti_{5/3}$]O_4/$LiMn_2O_4$ cells were constructed based on the following characteristics of the anode and cathode materials: (i) the anode Li[$Li_{1/3}Ti_{5/3}$]O_4 can be discharged to 150 mAh/g capacity, (ii) the cathode $LiMn_2O_4$ and $LiCoO_2$ can provide 120 mAh/g and 140 mAh/g [16,18] charge capacity, respectively. The ratio of the anode and cathode active materials were maintained as a slight excess of the anode active Li[$Li_{1/3}Ti_{5/3}$]O_4 in the cell configuration. The charge/discharge data for Li[$Li_{1/3}Ti_{5/3}$]O_4/$LiCoO_2$ and Li[$Li_{1/3}Ti_{5/3}$]O_4/$LiMn_2O_4$ cells are shown in Fig. 5. The voltages of the freshly assembled cell are in the range of 0.6–0.8 V. The average charge/discharge voltages for these two types of cells are around 2.4–2.5 V. As shown in Fig. 5b, the discharge capacity of the Li[$Li_{1/3}Ti_{5/3}$]O_4/$LiMn_2O_4$ cell fades quite quickly at an average rate of 0.34 mAh/g per cycle in the first 50 cycles. This is related to the degradation of the $LiMn_2O_4$ cathode [16]. However, the discharge capacity fading of the Li[$Li_{1/3}Ti_{5/3}$]O_4/$LiCoO_2$ cell is much lower, with an average rate of only 0.06 mAh/g per cycle. This suggests that the rechargeability of $LiCoO_2$ is better than that of $LiMn_2O_4$. Therefore, the contribution to the decline of the capacity is mainly due to the degradation of the cathode, since the Li[$Li_{1/3}Ti_{5/3}$]O_4 anode is very stable upon cycling. Although, the lithium ion cell with Li[$Li_{1/3}Ti_{5/3}$]O_4 as anode is structurally stable, its energy density is lower than that using a carbonaceous anode due to the relatively higher operating potential of the Li[$Li_{1/3}Ti_{5/3}$]O_4 anode (1.5 V vs. Li).

3.3. AC impedance determination of the Li[$Li_{1/3}Ti_{5/3}$]O_4 electrode

AC impedance spectra of the Li/Li[$Li_{1/3}Ti_{5/3}$]O_4 cell was obtained at the different discharged states. The cell was potentiostatically discharged from OCV (3.0 V) to 1.55 V, 1.5 V, and 1.2 V, respectively, and then equilibrated for 10 h. The AC impedance was performed at these conditioned potentials. The Nyquist plot are presented in Fig. 6. A single semicircle is displayed along the real axis in the high frequency range. At lower frequencies, a straight line inclines to the real axis with an angle of 45°, corresponding to the Warburg impedance.

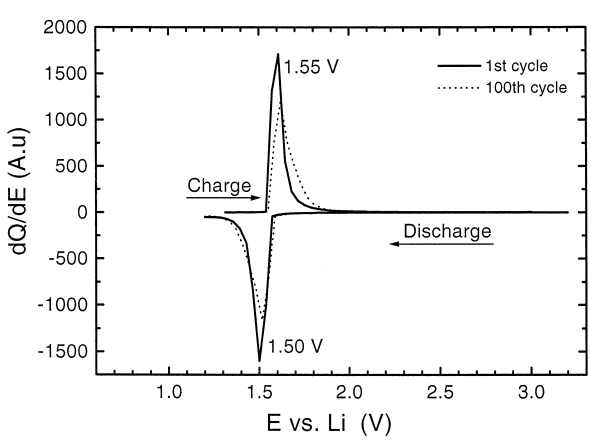

Fig. 4. Differential chronopotentiometric curves for Li/Li[$Li_{1/3}Ti_{5/3}$]O_4 cell in Fig. 3.

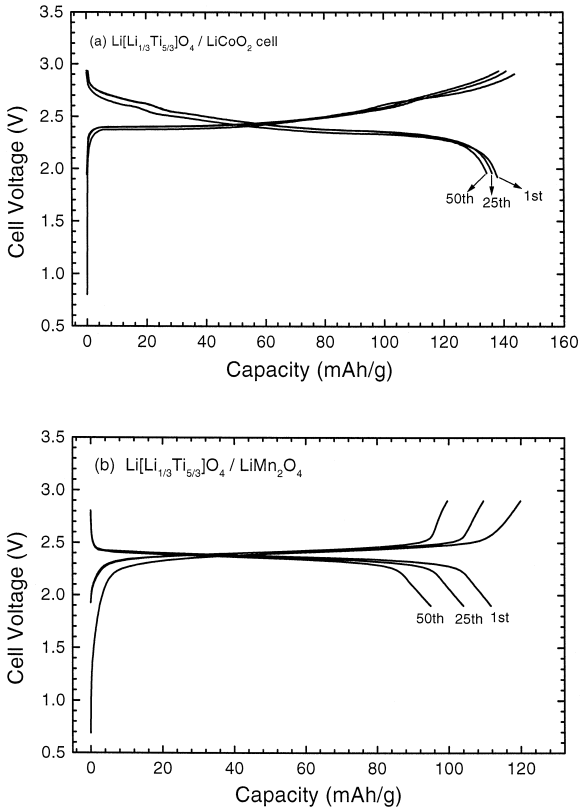

Fig. 5. The charge/discharge data of $Li[Li_{1/3}Ti_{5/3}]O_4/LiCoO_2$ and $Li[Li_{1/3}Ti_{5/3}]O_4/LiMn_2O_4$ cells. The cells were cycled between 1.9 V and 2.9 V at a constant current density of 0.15 mA/cm^2, corresponding to a rate of C/6. The capacities are based on the mass of the cathode active materials.

A second semicircle has been observed for AC impedance spectroscopy of the $Li/LiMn_2O_4$ system, which is attributed to the formation of a surface layer on the electrode due to the oxidation of the electrolyte on the surface of the highly charged $LiMn_2O_4$ electrode [19]. In the $Li/Li[Li_{1/3}Ti_{5/3}]O_4$ system, this second semicircle was not observed in the voltage range of OCV (3.0 V)–1.2 V, which is in the voltage window of the cycling of the $Li[Li_{1/3}Ti_{5/3}]O_4$ electrode. The equivalent circuit for the $Li/Li[Li_{1/3}Ti_{5/3}]O_4$ system is also shown in Fig. 6 as an inset, which consists of (i) faradic components: the charge-transfer resistance R_{CT}; the electrolyte resistance R_{EL} and the Warburg resistance Z_W. (ii) A non-faradic component: double layer capacitance C_{DL}. The exchange current density can be calculated from the following equation: $i_o = RT/nFR_{CT}$. The double layer capacitance (C_{DL}) also could be deduced from this semicircle according to: $C_{DL} = 1/R_{CT}\omega_{max}$. The kinetic parameters of $Li[Li_{1/3}Ti_{5/3}]O_4$ electrode are shown in Table 1. The charge-transfer resistance (R_{CT}) at 1.50 V (discharge plateau) and 1.20 V (deeply discharge state) are the same and higher than that at OCV and initial discharge state (1.55 V). The double-layer capacitance increases as lithium insertion proceeds and keeps constant

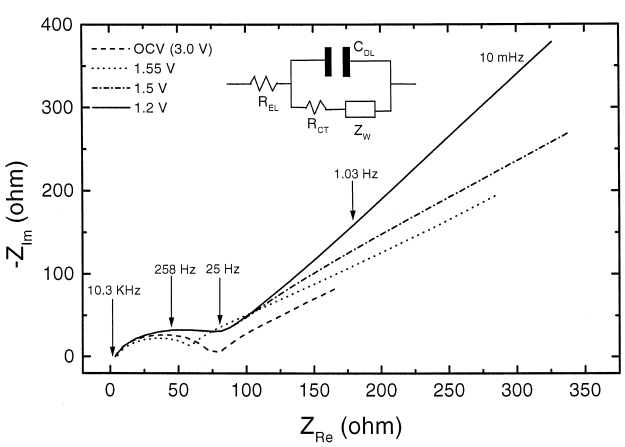

Fig. 6. AC impedance spectra of a $Li/Li[Li_{1/3}Ti_{5/3}]O_4$ cell obtained at different conditioned potentials.

Table 1
The kinetic parameters of the $Li[Li_{1/3}Ti_{5/3}]O_4$ electrode at different discharge states

Discharge state/kinetic parameters	OCV (3.0 V)	1.55 V	1.50 V	1.20 V
Charge-transfer resistance (R_{CT}, Ω/cm^2)	75.69	65.78	106	106
Exchange current density (i_o, A/cm^2)	3.39×10^{-4}	3.90×10^{-4}	2.42×10^{-4}	2.42×10^{-4}
Double-layer capacitance ($\mu F/cm^2$)	5.1	5.9	9.1	9.1

from 1.50 V (discharge plateau) to 1.20 V (cut-off voltage), indicating no change of the double-layer of the $Li[Li_{1/3}Ti_{5/3}]O_4$ electrode during this discharging process.

It has been determined that a passivation film forms on the surface of an anode such as carbon at the potential of ~ 0.8 V vs. Li/Li^+, which is caused by the solvent decomposition reaction. The passivation film compounds are complicated and only known to contain Li_2CO_3, C–H bonds and COOH groups [11]. When the passivation film forms on the surface of the anode in lithium ion cells, lithium ions have to diffuse through it. During long term cycling, this passivation film could be blocked and consequently, result in the formation of chemically unstable lithium powder or dendrites. From the result of the AC impedance spectra of $Li[Li_{1/3}Ti_{5/3}]O_4$ electrode, it seems that the $Li[Li_{1/3}Ti_{5/3}]O_4$ electrode is passivation free. From these results therefore, it appears that the passivation free $Li[Li_{1/3}Ti_{5/3}]O_4$ anode is much safer for battery operation than either lithium metal or carbonaceous anodes.

4. Conclusions

Spinel $Li[Li_{1/3}Ti_{5/3}]O_4$ was synthesised and its electrochemical properties in lithium cells were tested. The maximum amount of Li ions which can be inserted into $Li[Li_{1/3}Ti_{5/3}]O_4$ structure is limited to be about one Li ion per formula $Li[Li_{1/3}Ti_{5/3}]O_4$. $Li[Li_{1/3}Ti_{5/3}]O_4$ demonstrated a very stable characteristic for Li ion insertion and extraction without passivation. $Li[Li_{1/3}Ti_{5/3}]O_4/LiCoO_2$ and $Li[Li_{1/3}Ti_{5/3}]O_4/LiMn_2O_4$ cells provide an average operating voltage of 2.4–2.5 V with no safety concern. Further optimisation of the synthesis of $Li[Li_{1/3}Ti_{5/3}]O_4$ is needed to improve its electrochemical properties.

References

[1] J.B. Goodenough, A. Manthiram, B. Wnetrzewski, J. Power Sources 43–44 (1993) 269–275.
[2] R. Koksbang, J. Barker, H. Shi, M.Y. Saidi, Solid State Ionics 84 (1996) 1–21.
[3] T. Ohzuku, M. Kitagawa, T. Hirai, J. Electrochem. Soc. 137 (1990) 40–46.
[4] M.S. Whittingham, Prog. Solid State Chem. 12 (1978) 41.
[5] S. Subbarao, D.H. Shen, F. Deligiannis, C.K. Huang, G. Halpert, J. Power Sources 29 (1990) 579–587.
[6] T. Nagaura, JEC Battery Newsletter 2 (1991) 1–2.
[7] J.R. Dahn, U. Von Sacken, M.W. Juzkow, H. Al-janaby, J. Electrochem. Soc. 138 (1991) 2207–2211.
[8] D. Guyomard, M. Tarascon, J. Electrochem. Soc. 139 (1992) 937–948.
[9] J.M. Tarascon, D. Guyomard, J. Electrochem. Soc. 138 (1991) 2864–2868.
[10] K. Tokumitsu, A. Mabuchi, H. Fujimoto, T. Kasuh, J. Power Sources 54 (1995) 444–447.
[11] Y. Matsumura, S. Wang, J. Mondori, J. Electrochem. Soc. 142 (1995) 2914–2918.
[12] N. Imanishi, S. Ohashi, T. Ichikawa, Y. Takeda, O. Yamamoto, J. Power Sources 39 (1992) 185–191.
[13] M.M. Thackeray, J. Electrochem. Soc. 142 (1995) 2558–2563.
[14] M.M. Thackeray, A. de Kock, M.H. Rossouw, D. Liles, J. Electrochem. Soc. 139 (1992) 363–366.
[15] T. Ohzuku, A. Ueda, N. Yamamoto, J. Electrochem. Soc. 142 (1995) 1431–1435.
[16] G.X. Wang, D.H. Bradhurst, S.X. Dou, H.K. Liu, Proceeding of the 13th Annual Battery Conference on Applications and Advances, P375–380, IEEE 98TH8299, Long Beach, CA, USA, January, 1998.
[17] D.W. Murphy, R.J. Cava, S.M. Zahurak, A. Santoro, Solid State Ionics 9–10 (1983) 413.
[18] L. Gacctier, M. Meeccs, J. Scoyer, Progress in Batteries Materials, Vol. 16, IBA Tucson, AZ, USA, Meeting, P30–43, ITE-JEC Press, Printed in Japan, 1997.
[19] P. Arora, N.N. Popov, R.E. White, J. Electrochem. Soc. 145 (1998) 807–815.